# *Chapter 7: Evaluation of morphological changes of histopathological images of ovarian and breast cancer tissues and its correlation with their biochemical parameters*

## Abstract:

Ovarian and breast cancers have become the foremost cause of fatality and are frequently diagnosed among women in worldwide. Several factors have been found to be responsible for uncontrolled proliferation of epithelial cells of ovary and breast. Lipid peroxidation (LPO) is the result of increased oxidative stress in the cells that may be involved in many pathological deregulations including cancer, cell injury and aging. Various biomolecules like lipid, proteins etc. are considered to be damaged due to over production of reactive oxygen species (ROS) as a consequence of LPO. Malondialdehyde (MDA) is an important indicator of the lipid damage and produced as a by-product of LPO. The aim of the work is to do comparative evaluation of morphological features of dysplastic change of cells such as enlarge size, irregular shape, hyperchromatic nuclei etc. and its correlation with biochemical parameters. For determination of MDA level in serum of ovarian and breast cancer patients, LPO assay has been performed. The study comprised of 55 controls, 75 ovarian and 75 breast cancer patients. The results reveal that MDA levels, CA-125, WBC, are increased, while RBC, Haemoglobin (Hb) and platelets count decreased in cancer patients as compared to normal. For comparing morphological changes in cells, 5 normal and 5 cancerous tissues have been evaluated for ovarian and breast cancers.

## 7.1 Introduction:

Ovarian and breast cancer are the leading cause of cancer related death in women and the most lethal gynaecological malignancy in the developed world (Siegel *et al.,* 2015). Both the cancers have been reported to have a highest mortality rate. In 2015, an estimated 22,280 women were diagnosed with ovarian cancer in the worldwide. It is estimated that almost 14,240 deaths occur every year due to ovarian cancer. In 2015, 60,290 new cases of breast carcinoma were diagnosed in situ, 83% of which were ductal carcinoma in situ (DCIS) and 12% lobular carcinoma in situ (LCIS) in worldwide (Siegel *et al.,* 2015). Among all ovarian malignancies (80-90%), epithelial cell carcinoma is most frequent (Badgwell *et al.,* 2007; Tavassoli, 2003). Four most common cell types of

epithelial ovarian cancer are serous, mucinous, clear cell and endometrioid (Bell, 1991; Scully, 1995; Hennessy *et al.,* 2009); Romero and Bast, 2012).

The morbidity and mortality of ovarian cancer underscore the need for novel detection techniques (Siegel *et al.,* 2015).

**ROS Induce Lipid peroxidation:**

Oxidative stress is one of causative agent for cancer development. Oxidative stress occurs in the cell due to the production of ROS in cells. ROS oxidized the lipid to cause per oxidation of lipids for starting with the evolution of cancer. ROS is a key factor resulting in lipid peroxidation and hence oxidative stress. Reactive oxygen species are a type of oxygen-derived free radical whose role in cell injury is well established. ROS are the chemically reactive molecules carrying free radicals. High concentration of these oxygen free radicals can lead to oxidative damage (Hristozov *et al.,* 2001; Dix *et al.,* 1993). ROS includes free radicals such as superoxide anion ($O_2$-$^o$), per hydroxyl radical ($HO_2^o$), hydroxyl radical ($OH^o$) are produced during normal cellular metabolism (Salvador *et al.,* 2001; Riess *et al.,* 2004). Lipid peroxidation is a consequence of the action of reactive oxygen species (ROS) on polyunsaturated fatty acid (PUFA) and its degradation to MDA (Salganik, 2001). MDA is one of the by-products of lipid peroxidation and is commonly used as a key biomarker for lipid peroxidation. Degradation of lipid results in loss of PUFA in the plasma membrane. The weakening of plasma membrane increases the permeability of the outer mitochondrial membrane ((Kroemer, 2003; Newmeyer and Shelagh, 2003). In addition, it acts as a mutagen and has been shown to activate proto-oncogenes or tumor suppressor genes (von Sonntag,1987). Free radicals alter the activity of adjacent molecules, such as proteins, lipids, carbohydrates, nucleic acids, etc., which are key components of a structural and functional basis of cell and nuclei (Weinstein *et al.,* 2000). Cell injury caused due to the reactive oxygen species is well established.

**Mechanism of lipid per oxidation:**

In this process free radicals take electrons from the lipids in cell membranes, resulting in cell damage. ROS attacks PUFA in the plasma membrane to initiate series of

reaction to produce Malondialdehyde (MDA). This process proceeds by a free radical chain reaction mechanism. It mainly affects polyunsaturated fatty acids, as they contain reactive hydrogens containing methylene bridges (-CH2-) in between multiple double bonds. Free radical chain reaction consists of three general steps: initiation, propagation, and termination. Reactive oxygen species (ROS) is generated during normal cellular metabolism mostly in mitochondrial respiration during electron transport chain. However, they are degraded and removed by cellular defense systems (Hennig and Chow, 1998). Decreased scavenging agents of ROS may lead to an excess generation of free radicals and cause oxidative stress leading towards the wide variety of pathological processes such as cell injury, cancer, aging, and some neuro degenerative diseases (Barrera *et al.*, 2008; Rice-Evans and Burdon, 1993) as shown in figure 7.1.

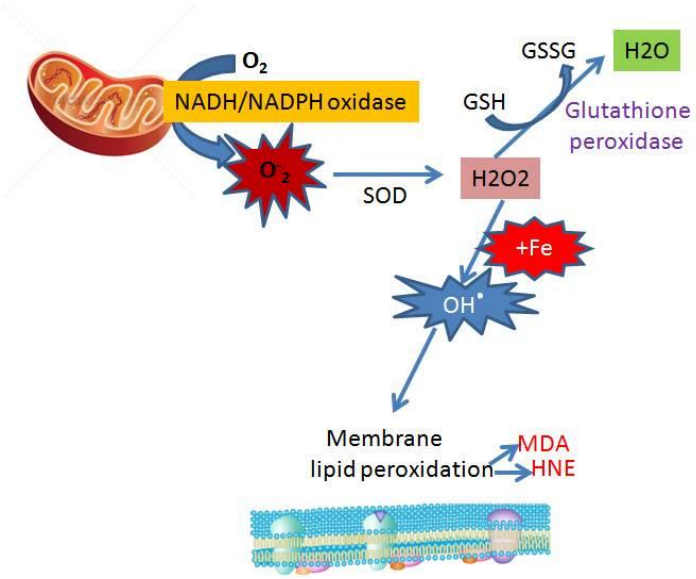


**Figure 7.1: Mechanism of lipid peroxidation.**

CA-125 is the most extensively studied biomarker for use in the possible early detection of ovarian carcinoma, and it has been proven to be valuable in both detection and disease monitoring. CA-125 is a high molecular mass glycoprotein, size ranging from 200-2000 kDa (Davis *et al.*, 1986). CA125 is expressed as a membrane bound protein at the surface of epithelial cells and released in soluble form in bodily fluids when over expressed. It has been indicated that CA-125 is a typical mucin, a glycoprotein, with a repeat of serine and threonine (O-linked) glycan chains (Lloyd *et al.*, 1997). CA-125 can

be present in higher concentration in blood serum of ovarian cancer cells compared to normal.

## 7.2 Materials and methods:

75 ovarian, 75 breast and 55 normal women with similar age group were included in the studies for biochemical examination from pathology department, S.S. Hospital and Research Institute, Patna. For the estimation of MDA levels, only 25 samples from each group have been included. For the study of morphological features of ovarian and breast cancer cells, each containing 5 normal and 5 cancerous tissues were collected. The image data has been obtained from examination of a breast and ovarian biopsy. The data gives the information about the breast and ovarian histology content, characteristics of nuclei. Accordingly, the data was transformed utilizing CAD for investigation.

### 7.2.1 Biochemical estimation:

**Serum separation**

The biochemical investigation has been performed after the intravenous blood sample collection through syringe from cancer patients. The blood collected in the vacutainer was allowed to stand at 37ºC for 1 hour. It was then centrifuged for 15 minutes at 3000 rpm (18 ºC). The tube was carefully taken without shaking and serum was pipetted out into microfuge tubes. The serum was stored in the deep freezer until further use.

#### 7.2.1.1 Hematological analysis:

Intravenous blood has been used for the estimation of Red Blood Cell (RBC) count, White Blood Cell (WBC) count, Haemoglobin (Hb) level, platelet count by standard procedures were assessed using cell counter (Medonic M-Series) in the pathology department, S.S. Hospital, and Research Institute, Patna (Bihar). To collect serum, the rest of the blood was centrifuged for 10 min at 3000 rpm as shown in figure 7.2.

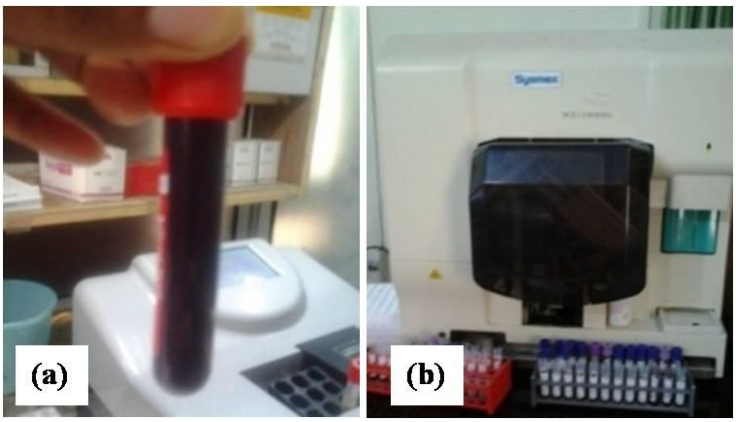


**Figure 7.2: Hematological test.**
(a) Tube contains blood. (b) Complete blood count analyzer.

### 7.2.1.2 CA-125 assay:

Blood samples collected from cancer patients were used for estimation of CA-125 (U/ml). CA-125 standard and test serum (100 µl) were pipetted in appropriate wells and then, enzyme conjugate reagent was dispensed into each wells. The solution was mixed well for 30 seconds and incubated at $37^0$C for 90 minutes. The wells were emptied and washed five times with wash buffer. 100µl of TMB Reagent was dispensed into each well and gently mixed for 10 seconds, then incubated at room temperature in the dark for 20 minutes. The reaction was stopped by adding stop solution to each well and colour change was observed from blue to yellow. Optical density was read at 450 nm with microtiter plate reader within 15 minutes. CA-125 was estimated from the serum with the help of ELISA reader (Monobind Inc.) as shown in figure 7.3.

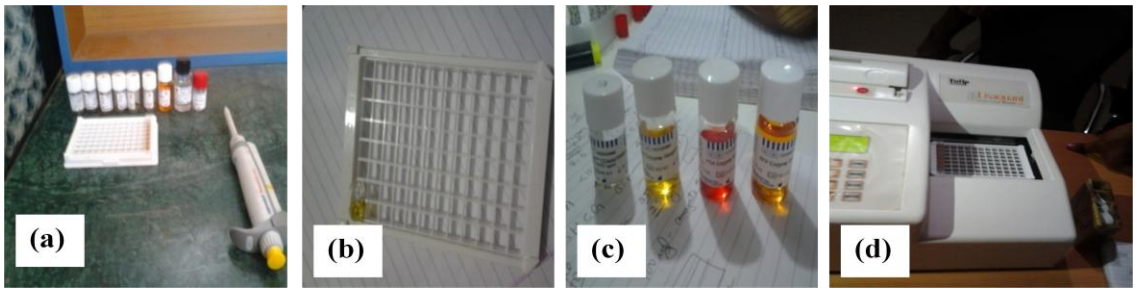


**Figure 7.3: Elisa Test**
(a) Elisa kit (b) Microtiter plate (c) Elisa Reagent (d) Elisa microplate reader.

### 7.2.1.3 Estimation of lipid peroxidation:

The 25 samples were taken from each group normal women, ovarian cancer and breast cancer patients included in the study for the estimation of LPO assay.

- **Requirements:** Test tube, 10% TCA, 0.675% TBA, Distilled water, Micropipette, micro tips.
- **Procedure: Stock for reagent:**
- **Trichloroacetic acid (TCA)**: 10gm of TCA is added in 100 ml of water to make 10% of TCA.
- **Thiobarbituric acid (TBA):** 0.675gm of TBA is added in 100 ml of distilled water to make 0.675% of TBA.

For the quantification of the end-products of lipid peroxidation certain diagnostic tests are available. For estimation of MDA thiobarbituric acid reactive substances (TBARS) assay is the most common test. In this assay, a fluorescent product is formed by the reaction of thiobarbituric acid with malondialdehyde. Reactive aldehyde such as MDA is the end products of lipid peroxidation. One of the most widely accepted assays for oxidative damage is the measuring the end products of lipid peroxidation. The estimation of lipid peroxidation of serum samples was done by taking the serum of control and cancer patients for different age groups. This method of Thiobarbituric Acid Reactive Substance (TBARS) was based on detection of MDA level in each serum samples. The level of lipid per oxidation in the serum was measured in term of Malondialdehyde (MDA; a broken down product of lipid peroxidation) content and determination were done by using the Thiobarbituric Acid (TBA) and Trichloroacetic Acid (TCA) reagents. A blood sample was centrifuged at 3000 rpm for 10 minutes to obtain serum.

For this, 2.5 ml of 10 % of trichloroacetic acid (TCA) was added to 0.5 ml of blank (Distilled water) and test serum of control and cancer patients. The reaction mixture was incubated for 15 minutes at 95°C followed by centrifugation at 3000 rpm for 10 minutes. The supernatant was collected, and 1 ml of 0.675% of thiobarbituric acid (TBA) was added and kept for incubation at 95°C for 15 minutes in water bath.

The pink colored reaction was obtained and optical density (OD) was measured with the help of Color Eye (IBL), colorimeter and the amount of TBARS were calculated (Ohkawa *et al*., 1979) as shown in table 7.1 and figure 7.4.

**Table 7.1: Sample preparation for the estimation of MDA by TBARS method.**

| | **Test** | **Blank** |
|---|---|---|
| TCA (10%) | 2.5ml | 2.5ml |
| Serum | 100 µl | _ |
| Distilled water | _ | 100 µl |
| **TBA** | 1.0 ml | 1.0 ml |

**Calculation:**

**5×5×Test O.D×4 /0.262 unit - nmol/µl**

**MDA range:**

Normal range- the value is between 15- 25 (nMol/ml).

Cancerous range- the value is between 25-50 (nMol/ml).

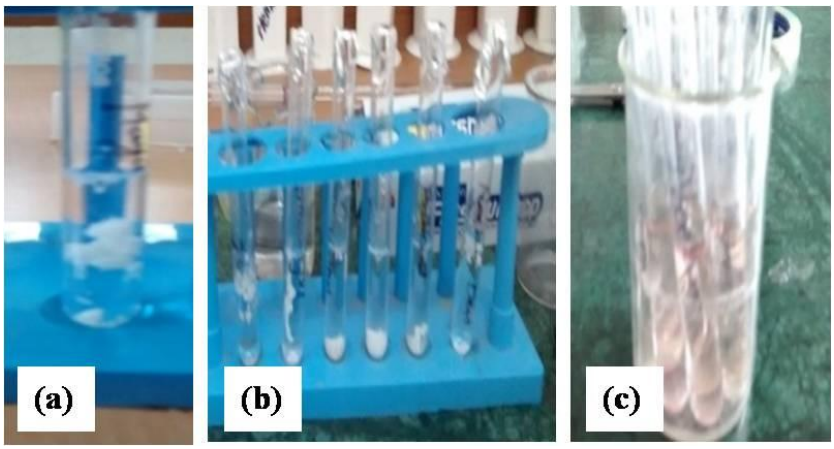


**Figure 7.4: Estimation of lipid peroxidation test.**
(a) TCA added to serum (b) Precipitation occurs (c) After adding TBA it gives pinkish color. (The thiobarbituric acid reacts with malondialdehyde to yield a fluorescent product).

### 7.2.2 Morphological Estimation:

Images were captured using Brightfield microscope (Olympus CH 20I) coupled with Magnus Pro 5 Megapixel camera and Top View software. For the study of morphological features of ovarian and breast cancer cells, tissues (each containing 5 normal and 5 cancerous) were collected. For this, tissues were fixed in 10% formalin and dehydrated in alcohol concentration in ascending order. Further, tissues were embedded in paraffin wax and the blocks were prepared. Sections of a thickness of 5-6 µm were cut using a microtome from the prepared blocks that were fixed on the slide with the help of Mayer's albumin. Slides were kept on xylene and were hydrated in alcohol concentration in descending order. The slides were stained using hematoxylin and dehydrated up to 70% alcohol. Further, the slides were stained with eosin and dehydrated up to 90% and 100% alcohol. After that, it is mounted with dibutyl phthalate in xylene (DPX).

#### 7.2.2.1 Preprocessing:

The main purpose of the pre processing stage is to reduce the background noise and to enhance the image to improve the image quality. In histopathology images, the blurriness, artifacts, weak boundary detection and overlapping problem occurred due to uneven staining of the slide. To remove the several artifacts presents during acquisition of the image, pre-processing has been done. The median filtering method is proposed to eliminate graininess (Lubawy and Skala, 2014).

#### 7.2.2.2 Segmentation:

In digital pathology, segmentation of histopathology sections is of prime importance due to the large variability of histopathological features of tissue. During image analysis, the segmentation process is an essential domain. It is used to locate objects and boundaries in an image (Sharma *et al.,* 2009). After the acquisition of the images, segmentation is performed for measurement of the cells in histopathological images. The basic purpose of segmentation is to extract the important features from the image (DiCataldo *et al.,* 2010).

### 7.2.2.3 Feature Extraction:

Image morphology is a very powerful tool for analyzing the shapes of the objects and to extract the image features, which are necessary for object recognition (Zhao *et al.*, 2015). The most significant portion of this work is the computation of features. After segmentation of image morphology based features have been extracted for further classification purpose.

These features provide information regarding the size and shape of cells. Features extraction of cells has been done from the segmented cells of the images. The quantification of these features helps to differentiate the cancerous cells from normal cells (Anuranjeeta *et al*., 2016).

Total eight (8) features (F1) to (F8) applied in this chapter are termed as count (F1), total area (F2), average size (F3), area fraction (F4), perimeter (F5), major axis length (F6), minor axis length (F7) and circularity (F8) respectively. The first four features count (F1), total area (F2), average size (F3) and area fraction (F4) is already discussed in chapter- 6, page no -180 and rest of the four features such as perimeter (F5), major axis length (F6), minor axis length (F7) and circularity (F8) are presented in chapter- 4, page no -104 -105 from the equations 4.3 to 4.6.

## 7.3 Results and discussion:

**Biochemical changes in histopathological images:**

Evaluation of biochemical parameters such as **(1)** MDA level **(2)** CA-125 level **(3)** RBC count **(4)** Hemoglobin level **(5)** WBC count **(6)** Platelet count is performed among normal women with ovarian and breast cancer patients. Comparative data of all biochemical parameters are shown in table 7.2 and figure 7.5 and figure 7.6.

The figure 7.5 (a) represents higher MDA (nMol/ml) levels for ovarian cancer (20.30±14.76) and breast cancer patients (21.94±14.07) as compared to the MDA levels in normal women (10.48±2.73) and shows a significant ($P< 0.0045$) difference. The figure 7.5(b) represents higher CA-125 (U/ml) levels for ovarian cancer (68.39±108.93) and breast cancer patients (35.84±20.71) as compared to CA-125 levels in normal women (30.00±24.06) and shows a significant ($P<0.0018$) P value.

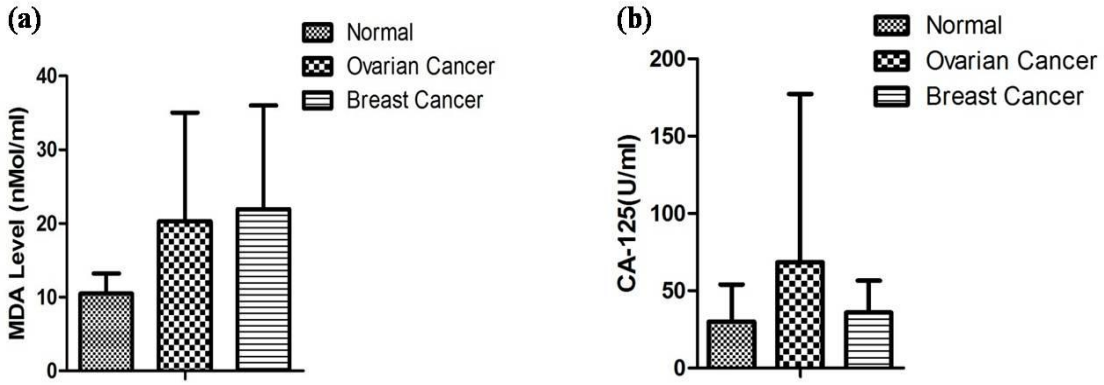


**Figure 7.5: Comparative results of biochemical parameter in normal, ovarian and breast cancer patients.**
(a) MDA level. (b) CA-125 level.

The figure 7.6 (a) represents lower RBC count (Million /µl) for ovarian cancer (3.99±0.61) and breast cancer patients (3.95±0.49) as compared to the RBC count in normal women (4.27±0.45) and shows a significant (P< 0.0036) difference. The figure 7.6 (b) represents lower Hemoglobin level (g/dl) for ovarian cancer (10.15±1.479) and breast cancer patients (9.88±1.28) as compared to the Hemoglobin level of normal women (11.06±1.115) and shows a significant (P< 0.0001) difference. The figure 7.6 (c) represents higher WBC count (thousand/µl) for ovarian cancer (11.30 ± 9.76) and breast cancer patients (10.21 ± 4.47) as compared to the WBC count of normal women (7.56 ± 2.19) and shows a significant (P<0.0078) difference. The figure 7.6 (d) represents lower Platelet count (thousand/µl) for ovarian cancer (225.5±96.19) and breast cancer patients (227.52 ± 116.11) as compared to the Platelet count of normal women (270.5 ± 80.37) and shows a significant (P<0.0223) difference.

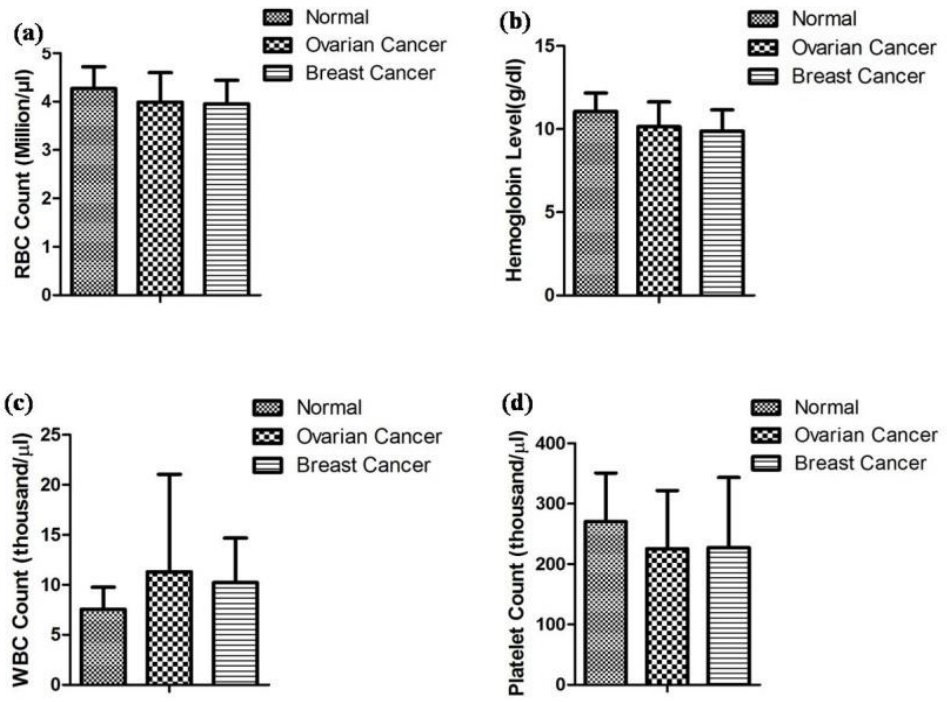


**Figure 7.6: Comparative results of biochemical parameter in normal, ovarian and breast cancer patients.**

(a) RBC count (b) Haemoglobin level (c) WBC count (d) and Platelet count

**Table 7.2: Comparative data of all biochemical parameters.**

| **Biochemical Parameter** | **Normal Women*** | **Ovarian cancer*** | **Breast cancer*** | ***p*-value** |
|---|---|---|---|---|
| MDA Level (nMol/ml) 25 | 10.48±2.73 | 20.30±14.76 | 21.94±14.07 | <0.0045 |
| CA-125 (U/ml) | 30.00±24.06 | 68.39±108.93 | 35.84±20.71 | <0.0018 |
| RBC count (Million /µl) | 4.27±0.45 | 3.99±0.61 | 3.95±0.49 | <0.0036 |
| Haemoglobin Level (g/dl) | 11.06±1.115 | 10.15±1.479 | 9.88±1.28 | <0.0001 |
| WBC count (thousand/µl) | 7.56 ± 2.19 | 11.30 ± 9.76 | 10.21 ± 4.47 | <0.0078 |
| Platelet count (thousand/µl) | 270.5 ± 80.37 | 225.5± 96.19 | 227.52±116.11 | <0.0223 |

The results presented here are expressed as *Mean ± S.D. Statistical analysis has been performed using Graph Pad Prism software (version 5.1). To perform unpaired, two-tailed students t-tests, p-value < 0.05 was used for significance.

The higher MDA level is shown in ovarian cancer patients as compared to normal persons in figure 7.5 (a). Most of the ovarian cancer is derived from epithelial cells, and ovarian cancer of epithelial origin has been asserted to produce abnormally high MDA (Sabuncu *et al.,* 2001). CA-125 is widely used as a specific and sensitive marker for early detection of ovarian cancer. The ovarian marker CA-125 level is too high in ovarian cancer patients as compared to healthy people. Being the member of mucin family, glycoprotein, CA-125 is usually embedded in plasma membrane however due to neoplasm development in epithelial ovarian cancer; it is relieved from the cell surface by the proteolytic action of the certain enzyme. The concentration of MUC16 increases in the peripheral blood due to which it acts as a prognostic marker for ovarian cancer. According to another reason, the release of CA-125 from the surface of the cell may also be due to loss of fluidity of plasma membrane which abets escaping of this transmembrane glycoprotein (Kobayashi *et al.,*1993). Higher MDA level in ovarian cancer patients corresponds to high CA-125 in blood serum in figure 7.5 (b).

RBC count provides enormous information on the effects of cancer and role played by oxidative stress (Bokemeyer *et al.,*2002) RBC count in figure 7.6 (a) and haemoglobin level in figure 7.6 (b) are lower in cancer patient than normal ones which mean less oxygen supply to tissue in cancer patient than in normal, this might be possible reason why ovarian cancer patients suffer great deal of oxidative stress which is due to incomplete electron transfer or reduction of oxygen by damaged mitochondria (Kaminski *et al.,*2002). Low level of Hemoglobin and RBC count in blood signifies that erythropoietin is hypoactive which means oxygen supply throughout the body is insufficient (Leyland-Jones *et al.,* 2005). Leukocytes are derived from hematopoietic stem cells in bone marrow. Due to the production of tumor antigens, it is anticipated that WBC count increases significantly. Levels of WBC count in ovarian patients are higher than normal in figure 7.6 (c) (Boon *et al.,* 1997). Platelets count lower in ovarian and breast cancer than normal in figure 7.6 (d) (Machlus *et al.,* 2014).

The MDA level and CA-125 biochemical parameters are found higher in cancerous tissue while the increase of other parameters like RBC count, WBC count, hemoglobin level, really do not signifies the presence of cancer, and it may be because of other diseases as well. MDA level can be used to increase the confidence level in cancer detection along with other parameters. However, more studies in this field of work are needed to be carried out to draw the concrete conclusion.

**Morphological changes in histopathological images**

On histopathological examination, morphological changes have been observed from the microphotograph of ovarian and breast cancer cells and compared with normal ovary and normal breast cells. The figure 7.7 (A1) photomicrograph of ovarian normal cells (A2) segmented image and (A3) outlines of segmented image and in figure 7.9 (A1) photomicrograph of breast normal cells (A2) segmented image and (A3) outlines of segmented image respectively, showed similar size and shape of cells, smooth nuclear border, a single nucleus with single nucleolus, large cytoplasm, fine chromatin are found. In breast cells presence of myoepithelial cells are observed.

Figure 7.8 (B1) show photomicrograph of ovarian cancer cells, (B2) segmented image and (B3) outlines of segmented image and in figure 7.10 photomicrograph of breast cancer cells (B1), segmented image (B2), and (B3) outlines of segmented image respectively, are mainly characterized by the dysplastic and architectural changes in cells which include increased mitotic count, multiple and large variably shaped nuclei/cells, coarse chromatin and irregular nuclear contour, hyperchromatic nuclei, nuclear invasion to the surrounding structure. Loss of myoepithelial cells in breast cancer cells has observed. Cells contain an increased number of nuclei with the clearly visible nucleolus. The mitotic count is elevated in number as compared to normal ovary. In the cancerous cells, cytoplasm is observed to be diffusing i.e. large cytoplasm to nucleus ratio. Spewing, blebbing, streaming, and irregularities of cytoplasm indicated that plasma membrane no longer provides support, and hence integrity of the cells is lost.

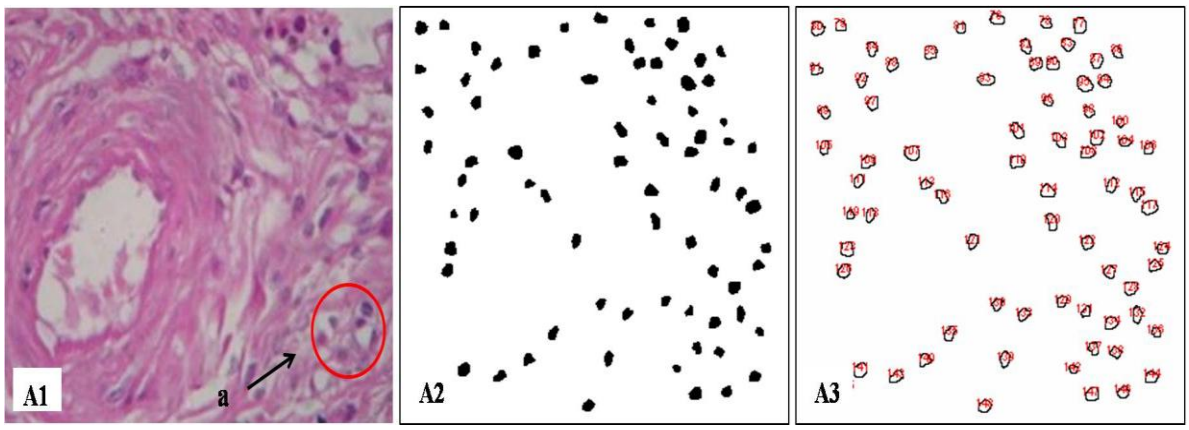


**Figure 7.7: Segmentation of normal ovary cells from the background of the image.**
A1: Microphotograph of original cross section of normal ovary tissue marked by (a) arrow showing similar in size and shape of cells, a single nucleus, large cytoplasm and smooth nuclear border. A2: Segmented image. A3: Outlines of the segmented image.

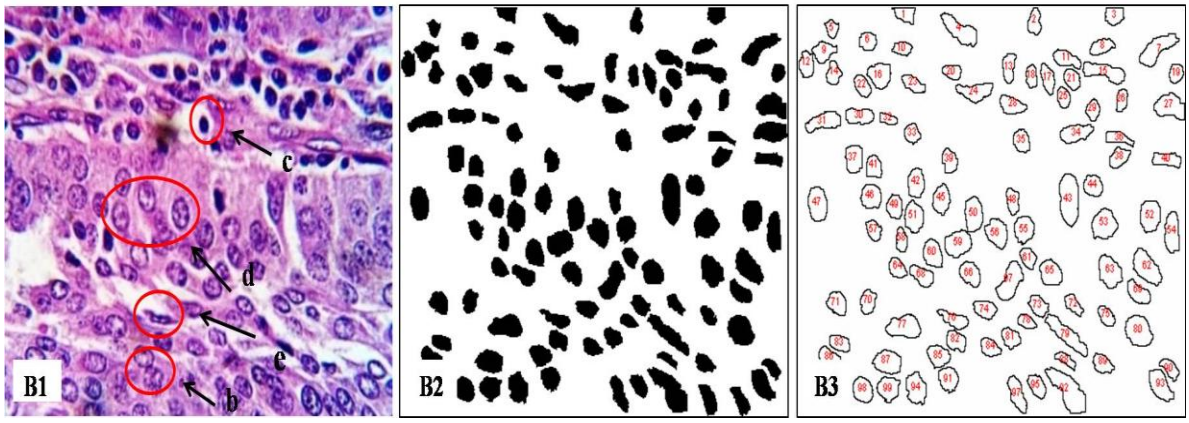


**Figure 7.8: Segmentation of malignant ovary cells from the background of the image.**
B1: Microphotograph of ovary papillary mucinous cyst adenocarcinoma marked by arrow (b) showing abnormal scattered, multinucleate cells and higher mitotic count, marked by arrow (c) hyperchromatic nuclei stained dark blue, marked by arrow (d) few germinal epithelial cell are enlarged with more nucleoli and per chromatin in nature, marked by arrow (e) diffused cytoplasm showing fusiform cells are significant feature of this stage. B2: Segmented image. B3: Outlines of a segmented image.

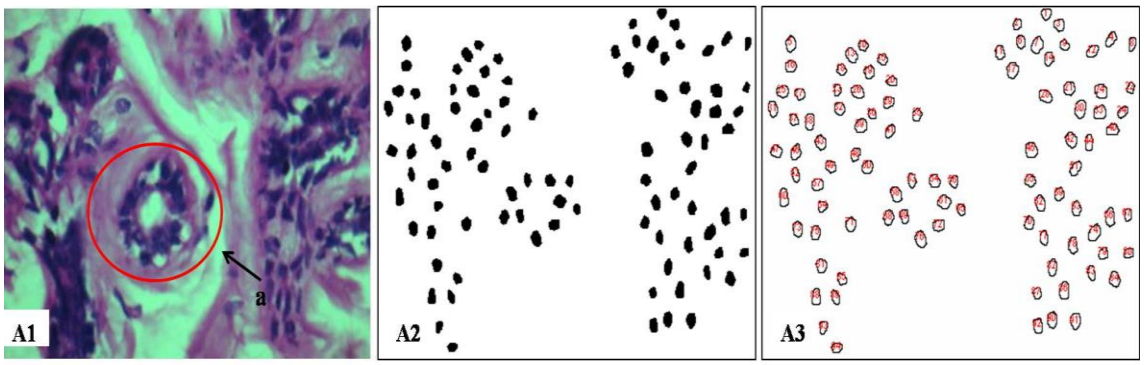


**Figure 7.9: Segmentation of normal breast cells from the background of the image.**
A1: Microphotograph of original section of normal breast tissue marked by an arrow (a) showing normal clusters of glands in the fibrous stroma, similar in size and shape of cells, a single nucleus, large cytoplasm, smooth nuclear border. A2: Segmented image A3: Outlines of the segmented image.

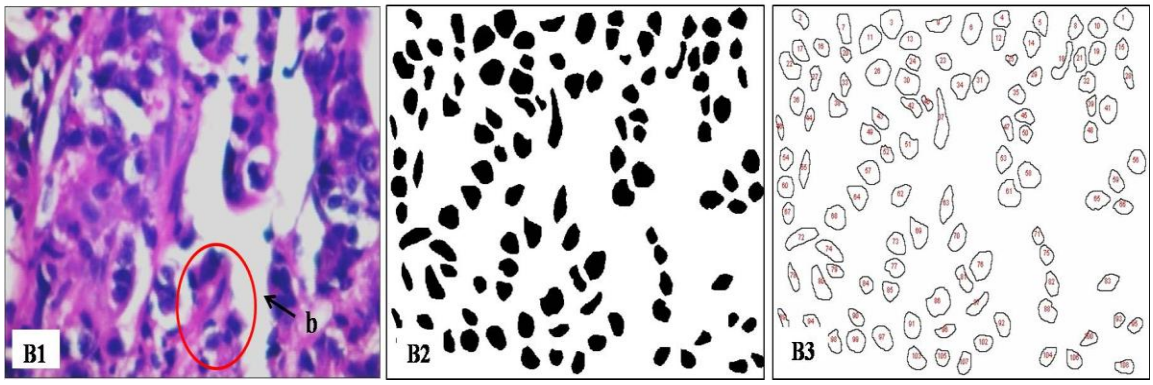


**Figure 7.10: Segmentation of malignant breast cells from the background of the image.**
B1: Microphotograph of original breast lump Infiltrating Ductal Carcinoma grade II marked by an arrow (b) showing the cells show pleomorphism and hyperchromatic nuclei. B2: Segmented image (B3) Outlines of the segmented image.

Evaluation of morphological features such as count (F1), total area (F2), average size (F3), area fraction (F4), perimeter (F5), major axis length (F6), minor axis length (F7) and circularity (F8) is performed among normal ovary and breast cells with ovarian and breast cancer cells. The figure 7.11(a) represents lower number of cell counts for normal ovary cells (80± 6.78) and normal breast cells (85.60±9.31) as compared to the cell counts for ovarian cancer cells (116.±16.56) and breast cancer cells (114.20±11.88) respectively and shows a significant ($P < 0.0029$) difference in table 7.3.

The figure 7.11 (b) represents lower value of total area (pixels$^2$) for normal ovary cells (9874.2±5303.12) and normal breast cells (11516.8±1967.98) as compared to the total area of ovarian cancer cells (29553.8±4233.54) and breast cancer cells (39951.2±1143.2) respectively and shows a significant (P< 0.0006) difference. The figure 7.11(c) represents higher value of average size (pixels) of ovarian cancer cell (261.55±68.49) and breast cancer cells (351.83±107.85) as compared to the average size of normal ovarian cells (119.89±54.89) and normal breast cells (135.27±21.71) respectively and shows a significant (P< 0.0023) difference. The figure 7.11(d) represents the higher value of area fraction (%) of ovarian cancer cell (18.22±4.09) and breast cancer cells (14.68±4.20) as compared to the area fraction for normal ovarian cell (5.88±0.89) and normal breast (9.03±1.54) respectively and shows a significant (P< 0.0226) difference.

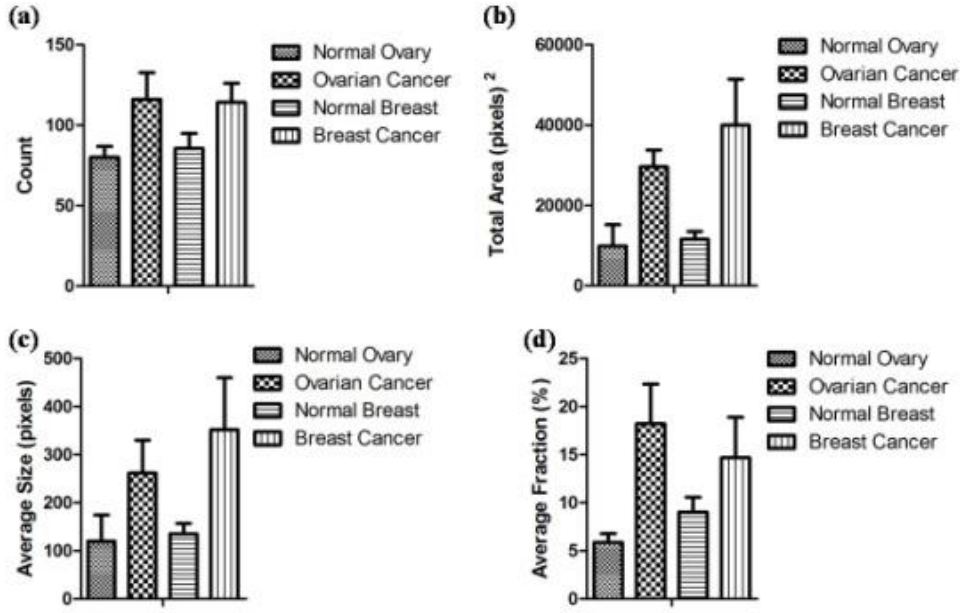


**Figure 7.11: Comparative results of features of normal ovary cells, ovarian cancer cells, normal breast cells and breast cancer cells.**

(a) Count (F1). (b) Total area (F2). (c) Average size (F3). (d) Area fraction (F4).

The figure 7.12 (a) represents the lower value of perimeter (pixels) for normal ovary cells (40.67±9.04) and normal breast cells (45.41±4.91) as compared to the perimeter for ovarian cancer cells (64.46±10.07) and breast cancer cells (74.19±10.40) respectively and shows a significant (P< 0.0005) difference. The figure 7.12 (b) represents higher value of major axis length (pixels) for ovarian cancer cell (23.44±3.87) and breast cancer cells (26.80±3.22) as compared to the major axis length for normal ovarian cell (14.29±2.82) and normal breast cells (16.20±1.93) respectively and shows a significant (P< 0.0002) difference. The figure 7.12 (c) represents higher value of minor axis length (pixels) for ovary cancerous cell (13.93±1.39) and breast cancer cell (16.23±2.84) ) as compared to the minor axis length for normal ovary cells (10.05±2.54) and normal breast cells (10.51±0.56) respectively and shows a significant (P< 0.0174) difference. The figure 7.12 (d) represents the value of circularity is nearly to 1(one) for normal ovary cells, (0.85±0.03) and normal breast cells (0.81±0.04) show that it circular in structure. The value is near to 0 (Zero) for elongated cells as compare to for ovary cancerous cell (0.77±0.03) and breast cancer (0.72±0.04) respectively, which show that it is less circular. This shows a significant (P< 0.0165) difference.

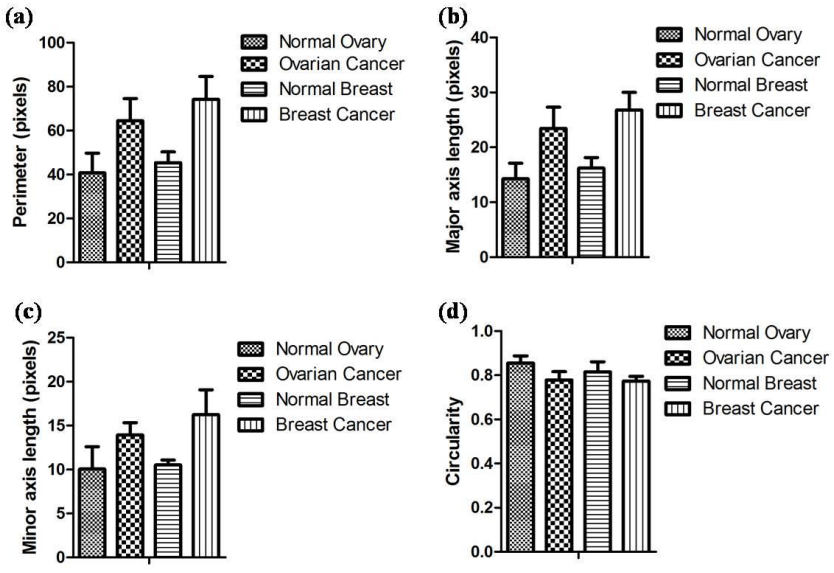


**Figure 7.12: Comparative results of features of normal ovary cells, ovarian cancer cells, normal breast cells and breast cancer cells.**

(a) Perimeter (F5). (b) Major axis length (F6). (c) Minor axis length (F7). (d) Circularity (F8).

Table 7.3 represents a significant difference for all the features count of cells (F1), total area (F2), average size (F3), area fraction (F4), perimeter (F5), major axis length (F6), minor axis length (F7) and circularity (F8).

**Table 7.3: Comparative data of all morphological parameters of an average value of five (5) sets of images in each group**

| S. No. | Morphological Features | Ovarian cells | | |
|---|---|---|---|---|
| | | **Normal*** | **Cancerous*** | **p-value** |
| F1 | Count | 80± 6.78 | 116.±16.56 | <0.0020 |
| F2 | Total area (pixels$^2$) | 9874.2±5303.12 | 29553.8±4233.54 | <0.0002 |
| F3 | Average size (pixels) | 119.89±54.89 | 261.55±68.49 | <0.0069 |
| F4 | Area fraction (%) | 5.88±0.89 | 18.22±4.09 | <0.0002 |
| F5 | Perimeter (pixels) | 40.67±9.04 | 64.46±10.07 | <0.0044 |
| F6 | Major axis length (pixels) | 14.29±2.82 | 23.44±3.87 | <0.0027 |
| F7 | Minor axis length (pixels) | 10.05±2.54 | 13.93±1.39 | <0.0174 |
| F8 | Circularity | 0.85±0.03 | 0.77±0.03 | <0.0083 |
| **S. No.** | **Morphological Features** | **Breast cells** | | |
| | | **Normal*** | **Cancer tissue*** | **p-value** |
| F1 | Count | 85.60±9.31 | 114.20±11.88 | <0.0029 |
| F2 | Total area (pixels$^2$) | 11516.8±1967.98 | 39951.2±1143.2 | <0.0006 |
| F3 | Average size (pixels) | 135.27±21.71 | 351.83±107.85 | <0.0023 |
| F4 | Area fraction (%) | 9.03±1.54 | 14.68±4.20 | <0.0226 |
| F5 | Perimeter (pixels) | 45.41±4.91 | 74.19±10.40 | <0.0005 |
| F6 | Major axis length (pixels) | 16.20±1.93 | 26.80±3.22 | <0.0002 |
| F7 | Minor axis length (pixels) | 10.51±0.56 | 16.23±2.84 | <0.0174 |
| F8 | Circularity | 0.81±0.04 | 0.72±0.04 | <0.0165 |

The results presented here are expressed as *Mean ± S.D. The results are statistically analyzed using Graph Pad Prism software (version 5.1). To perform unpaired, two-tailed students t-tests, $p$ –value <0.05 is considered significant.

Morphological changes in histopathological images of normal ovary (figure 7.7) and ovarian cancer in (figure 7.8) and normal breast (figure 7.9), breast cancer in (figure 7.10) respectively. In cancerous cells all are having increase count of cells, total area, average size, area fraction in figure 7.11 (a)-7.11 (d), and perimeter, major axis length, minor axis length and elongated shape (less circularity) in figure 7.12 (a) -7.12 (d) as compared to normal cells and yielded significant differentiation between normal and cancerous cells as shown in table 7.3. This is due to the reason that normal cells grow and divide when they receive signals from the surrounding cells and does not show contact inhibition phenomenon while malignant cells have uncontrolled cell division and grow faster (Kasmin *et al.,* 2012). Whereas normal cells undergo through aging and senescence process, as well as repair their physiological and chromosomal abnormalities (e.g. apoptosis) while cancerous cells show neither repair nor induce apoptosis. Normal cells become specialized or mature so that they can carry out their function in the body. While malignant cells often reproduce very quickly and do not exhibit mature phenotypes (Chen *et al.,* 2015). Hyperchromatic nuclei in cancer cells show the presence of high amount of deoxyribose nucleic acids (DNA) or an increase of nucleoprotein synthesis in the cancer cells, resulting in the larger nucleolus and dark-staining nuclei referred as hyperchromatism (Zhao and Murphy, 2007). The normal cells are found to be circular while cancerous cells are elongated, distorted or blebs shaped in figure 7.12 (d) that become physiologically non functional. Such types of shapes can be useful for cancerous cells to exhibit random migration i.e. metastasis (Belsare and Mushrif, 2012). The irregular and elongated shape help cancer cells to move from one place to another. In normal tissues, the cells stay together adheres to each other through specific microstructures that assist in governing the cellular function.

ROS is the initiative agent for lipid peroxidation and generated during electron transport chain in mitochondria. The lipid peroxidation involves degradation of lipid molecules in plasma or organelles membrane leading to changes in the permeability and fluidity of the membrane lipid bilayer and dramatically alters cell integrity. Increased ROS has been associated with apoptosis and cell proliferation by interacting with cell signalling cascade.

Increasing levels of ROS leads to damage extracellular matrix and hence, damages protein as well (Marnett, 1999). This might lead to possibilities of glandular loss. Increase in nucleus cytoplasm ratio, the non uniform cellular structure of cells is also observed in the association of high lipid peroxidation. However, oxidative stress is directly related to necrosis and apoptosis which manifests several malfunctions in the body.

## 7.4 Conclusion:

Structure based change in morphological features of ovarian and breast cancer cells as compare to normal have been calculated and their relation to increasing level of MDA has been included in this study. The losses of plasma membrane integrity of the cell are observed in the histopathological study. The predictive output for ovarian cancer can be derived with the help of analysis of MDA along with CA-125 and histological studies. Morphology-based features of ovarian and breast cancer have the higher count of cells, total area, average size, area fraction, perimeter, major axis length, minor axis length and lower circularity (elongated shape) as compared to normal cells and yielded significant differentiation between normal and ovarian and breast cancerous cells. Effects of oxidative stress on ovarian cancer should be taken seriously and worked more to mitigate its disastrous effects. All such parameters have been evaluated and studied extensively to establish a correlation between oxidative stress, CA-125, RBC count, Haemoglobin level, WBC count and platelets counts in ovarian cancer patients with normal persons. A combinatorial approach including image based tissue analysis as well as the biochemical examination is required to be established for cancer detection. Further, it requires the suitability and validation of such approach for the detection of other various cancerous tissues.